

Copyright © 2014 IEEE. Reprinted from Satinder Singh Gill, Brent R. Petersen, “Performance dependence of line-of-sight multiuser multi-input multi-output system on allocated user bandwidth in an office environment,” *2014 International Conference on Advances in Computing, Communications and Informatics, ICACCI 2014*, (Delhi, India), pp. 1775-1780, Sept. 24-27, 2014.

This material is posted here with permission of the IEEE. Internal or personal use of this material is permitted. However, permission to reprint/republish this material for advertising or promotional purposes or for creating new collective works for resale or redistribution must be obtained from the IEEE by sending a blank email message to pubs-permissions@ieee.org.

By choosing to view this document, you agree to all provisions of the copyright laws protecting it.

Performance Dependence of Line-of-Sight Multiuser Multi-Input Multi-Output System on Allocated User Bandwidth in an Office Environment

Satinder Singh Gill and Brent R. Petersen
 Department of Electrical and Computer Engineering
 University of New Brunswick
 Fredericton, Canada

Abstract—In this paper, the line-of-sight (LOS) multiuser multi-input multi-output (MU-MIMO) system present in an office environment is considered. The major idea behind the proposed work is to demonstrate the effect of allocated user bandwidth on the performance of a bandlimited MU-MIMO system in an office environment. The hypothesis is proposed to estimate the average MU-MIMO bandwidth of an office environment. The computer simulation results for a 2 × 2 LOS MU-MIMO scenario show great improvement in the performance of the MU-MIMO system for optimal user bandwidth allocation. Finally, the presented measurement results attest the MU-MIMO system theoretical and simulation performance improvement predictions.

Index Terms—MIMO, rician channels, line-of-sight propagation, multiuser channels.

I. INTRODUCTION

Multiuser multi-input multi-output (MU-MIMO) systems are well known to provide a capacity improvement as compared with single antenna systems [1]. The use of multiple antennas offers a new dimension, a spatial dimension, which can be exploited to provide enhanced communication performance. However, the capacity improvement through the use of MU-MIMO systems is highly dependent on the MU-MIMO channel characteristics [15]. These characteristics mainly include MU-MIMO channel scattering richness, transmit and receive array inter-antenna separation, as well as the distance between transmit and receive antenna arrays. Theoretically, the capacity improvement through the use of MU-MIMO systems is proportional to the minimum of the number of transmit and receive antennas [10]. In a typical outdoor urban environment, the presence of rich multipath scattering leads to a variation of amplitude and phase angles of signals at different receive antennas, leading close to predicted theoretical capacity improvements. Unfortunately, in a typical rural outdoor and urban indoor environment, the transmit signal reaches the receive antenna mainly through a line-of-sight (LOS) path. If the inter-antenna separation is small, the linear dependence of the LOS rays' phases is high, resulting in degraded MU-MIMO performance.

In the past, much research has been presented to maximize the LOS MU-MIMO system performance. Most of the presented research focuses on achieving performance improvement through the use of antenna element positioning, antenna design and antenna polarization. All of this presented

research, [11], [13] and [15], considers antenna separation on different scales of carrier wavelength (i.e. full carrier wavelength, half carrier wavelength or quarter carrier wavelength). Zhu et al. consider antenna separation on the scale of symbol wavelength named signaling wavelength to improve channel matrix invertibility of space-time receivers for LOS environments [10]. Their work reveals that for LOS environments antenna separation on the scale of symbol wavelength can lead to improved performance as compared to separation on the scale of carrier wavelength. This hints at the dependence of LOS MU-MIMO system performance on the allocated user bandwidth.

In this paper, we investigate the average MU-MIMO bandwidth of an office environment. Further, we investigate the performance of a MU-MIMO system for different bandwidth conditions.

The rest of the paper is organized as follows: the next section presents the MU-MIMO system model which is followed by the MU-MIMO bandwidth analysis section. Thereafter, simulation results are presented which are followed by the MU-MIMO measurement results.

II. MU-MIMO SYSTEM MODEL

We consider a pure LOS MU-MIMO communication system consisting of M portable users each having single transmit antenna and one receiver consisting of N receive antennas. For simplicity, we assume that channel does not change over the interval of a transmission time and also the channel is assumed to be narrowband and frequency flat. In the frequency domain the input-output relationship for the MU-MIMO system can be modeled as

$$\mathbf{Y}(f) = \mathbf{H}(f)\mathbf{X}(f) + \mathbf{n}(f), \quad (1)$$

$$\begin{pmatrix} Y_1 \\ Y_2 \\ \cdot \\ Y_N \end{pmatrix} = \begin{pmatrix} H_{11} & H_{12} & \cdot & H_{1M} \\ H_{21} & H_{22} & \cdot & \cdot \\ \cdot & \cdot & \cdot & \cdot \\ H_{N1} & H_{N2} & \cdot & H_{NM} \end{pmatrix} \begin{pmatrix} X_1 \\ X_2 \\ \cdot \\ X_M \end{pmatrix} + \begin{pmatrix} n_1 \\ n_2 \\ \cdot \\ n_N \end{pmatrix}, \quad (2)$$

where \mathbf{Y} denotes the N -dimensional received signal vector, \mathbf{H} denotes the $N \times M$ dimensional channel transfer function matrix (i.e. H_{NM} denotes the channel transfer function between the M^{th} portable user and the N^{th} receive antenna), \mathbf{X} denotes the M -dimensional transmitted signal vector and \mathbf{n} denotes the N -dimensional independent identically distributed zero-mean, uncorrelated complex baseband Gaussian noise vector.

In the pure LOS environment the time-invariant channel impulse response can be modeled as [6]

$$h(\tau) = a_i \delta(\tau - \tau_i), \quad (3)$$

where $h(\tau)$ denotes the time-invariant channel impulse response, a_i denotes overall attenuation between transmit antenna to receive antenna on the i^{th} path and τ_i denotes propagation delay between transmit antenna and receive antenna on the i^{th} path. The channel transfer function H which is obtained by taking Fourier transform of the channel impulse response can be modeled as

$$H = \int_{-\infty}^{\infty} h(\tau) e^{-j2\pi f \tau} d\tau, \quad (4)$$

$$H = a_i e^{-j2\pi f \tau_i}. \quad (5)$$

Therefore the channel transfer function matrix for pure LOS MU-MIMO can be modeled as

$$\mathbf{H} = \begin{bmatrix} a_{11} e^{-j2\pi f \tau_{11}} & \dots & a_{1M} e^{-j2\pi f \tau_{1M}} \\ \vdots & \ddots & \vdots \\ a_{N1} e^{-j2\pi f \tau_{N1}} & \dots & a_{NM} e^{-j2\pi f \tau_{NM}} \end{bmatrix}, \quad (6)$$

where a_{NM} denotes the overall attenuation between the portable user M and receive antenna N , τ_{NM} denotes the propagation delay between portable user M to receive antenna N and f denotes the baseband frequency of operation.

Now in an office environment when receiving antennas are placed close to each other, the relative differences in magnitude response of a single LOS path between portable users and receive antennas is almost identical [10]. However, due to the time delay between different paths a phase offset exists between different paths. Therefore, to simplify the presentation of results the channel transfer function matrix for MU-MIMO system can be modeled as

$$\mathbf{H} = \begin{bmatrix} e^{-j2\pi f \tau_{11}} & \dots & e^{-j2\pi f \tau_{1M}} \\ \vdots & \ddots & \vdots \\ e^{-j2\pi f \tau_{N1}} & \dots & e^{-j2\pi f \tau_{NM}} \end{bmatrix}. \quad (7)$$

This is acknowledged to be an approximation of channel transfer function matrix but in a limited space office environment this does not significantly change the results. Therefore in the remainder of this paper the channel transfer function matrix for the MU-MIMO system is represented using phase offsets only.

III. MU-MIMO BANDWIDTH ANALYSIS

We divide this section into two subsections: in the first subsection the dependence of the multiuser spatial signature combination on allocated user bandwidth is revealed and in the second subsection a 2×2 LOS MU-MIMO channel transfer function matrix is investigated to derive the relationship between the allocated user bandwidth and the MU-MIMO system performance.

A. Multiuser Spatial Signature Resolvability

We start our analysis with a simple multi-user multi-input single-output (MU-MISO) system present in a particular office environment. The MU-MISO system scenario is depicted in Fig. 1 which shows two LOS propagation paths from two portable users to same receive antenna. The equivalent system is depicted in Fig. 2. Considering the aforementioned pure delay LOS scenario, the spatial signature combination at the input of the bandlimiting receiver filter can be modeled as

$$h(\tau) = \delta_1(\tau - \tau_{11}) + \delta_2(\tau - \tau_{12}), \quad (8)$$

where $h(\tau)$ is the spatial signature combination at the input of the bandlimiting filter, $\delta_1(\tau)$ is the impulse signal transmitted by first user, $\delta_2(\tau)$ is the impulse signal transmitted by second user, τ_{11} and τ_{12} denote the propagation delays from first and second user antenna to receive antenna respectively.

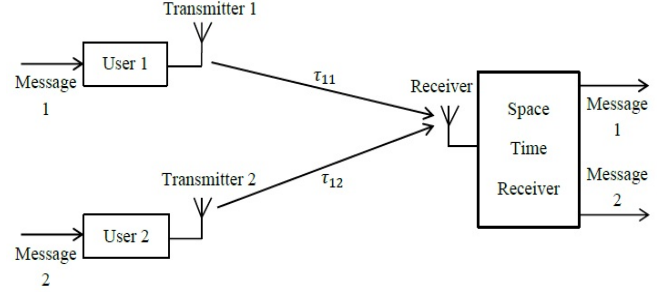


Fig. 1. MU-MISO system

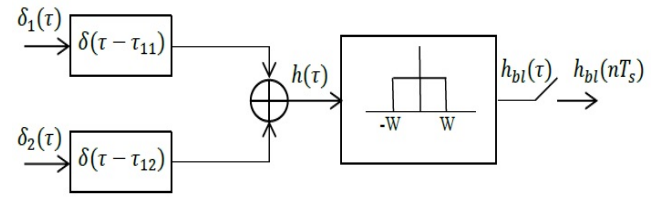


Fig. 2. Equivalent MU-MISO system

The output of the band-limiting filter is modeled as

$$h_{bl}(\tau) = 2W \text{sinc}(2W\tau - 2W\tau_{11}) + 2W \text{sinc}(2W\tau - 2W\tau_{12}), \quad (9)$$

where $\text{sinc}(\cdot)$ is the normalized mathematical sinc function.

The output of the sampler can be modeled as

$$h_{bl}(nT_s) = 2W \text{sinc}(2WnT_s - 2W\tau_{11}) + 2W \text{sinc}(2WnT_s - 2W\tau_{12}), \quad (10)$$

where T_s is the Nyquist sampling period and W is the one-sided baseband bandwidth. Assuming that each user has been allocated a complex baseband bandwidth of $2W$ Hz and using the Nyquist sampling criterion; equation (10) can be rewritten as

$$h_{bl}(nT_s) = 2W \text{sinc}(n - 2W\tau_{11}) + 2W \text{sinc}(n - 2W\tau_{12}), \quad (11)$$

where $h_{bl}(\tau)$ is the spatial signature combination at the output of the band-limiting filter and $h_{bl}(nT_s)$ is the spatial signature combination at the output of the sampler. The closer examination of (11) reveals that for a bandlimited MU-MIMO system the spatial signature combination is dependent on individual portable user propagation delays and the allocated portable user bandwidth.

B. Average MU-MIMO Bandwidth of an Office Environment

As discussed in the previous section for the LOS MU-MIMO systems the resolvability of the impulse response is guided by the propagation delay among portable users and receive antennas. The propagation delay in-turn depends upon the physical location of the portable users and receive antennas within an office environment, which is eventually guided by the volume of an office environment. Therefore, we can say that for an LOS MU-MIMO system impulse response resolvability is controlled by the volume of an office environment.

The impulse response between portable user M and receive antenna N for a bandlimited MU-MIMO system can be modeled as

$$h_{NM}(\tau) = 2W \text{sinc}(2W\tau - 2W\tau_{NM}). \quad (12)$$

Therefore, the transfer function between portable user M and receive antenna N in the frequency domain can be modeled as

$$H = \text{rect}\left(\frac{f}{2W}\right) e^{-j2\pi f \tau_{NM}}, \quad (13)$$

where $\text{rect}(\cdot)$ denotes the rectangular unity area unity amplitude pulse centered at zero. Therefore, the transfer function matrix for a 2×2 bandlimited MU-MIMO system can be modeled as

$$\mathbf{H} = \begin{bmatrix} \text{rect}\left(\frac{f}{2W}\right) e^{-j2\pi f \tau_{11}} & \text{rect}\left(\frac{f}{2W}\right) e^{-j2\pi f \tau_{12}} \\ \text{rect}\left(\frac{f}{2W}\right) e^{-j2\pi f \tau_{21}} & \text{rect}\left(\frac{f}{2W}\right) e^{-j2\pi f \tau_{22}} \end{bmatrix}. \quad (14)$$

For MU-MIMO systems the performance quality can be judged by the condition number of the baseband channel matrix. The closer the condition number gets to one better the expected system performance would be [15]. The best situation for the channel matrix in (14) to have a condition number equal to one is that all the columns or rows are orthogonal to each other. For channel transfer function matrix presented in (14), this can be represented as

$$e^{-j2\pi f (\tau_{21} + \tau_{12} - \tau_{11} - \tau_{22})} = -1, \quad (15)$$

$$|(\tau_{11} - \tau_{12} + \tau_{22} - \tau_{21})| = \frac{0.5}{f}. \quad (16)$$

Equation (16) states that for given values of propagation delays the MU-MIMO system performance can be improved by allocating appropriate user bandwidth to the given MU-MIMO system. In addition to this, it clearly shows the inverse relationship between the required MU-MIMO bandwidth and difference among propagation delays (i.e. if difference between propagation delays is small required MU-MIMO bandwidth is large and vice-versa). Since the propagation delays depend upon the location of the portable users and receive antennas within an office environment, which in turn is controlled by the volume of an office environment therefore (16) can be used to estimate the average MU-MIMO bandwidth of a given office environment. Unfortunately the relationship between the average MU-MIMO bandwidth and volume of an office environment is not directly evident from (16). However the closer look at (16) states that if the difference among propagation delays from different portable users to same receive antenna is maximized then bandwidth requirement would be decreased and vice-versa. Therefore, we propose a hypothesis which states that the average MU-MIMO bandwidth of an office environment B_{avg} , is inversely proportional to the maximum possible propagation delay between portable user and receive antenna. This can be represented as

$$B_{avg} = \frac{1}{\tau_{max}}, \quad (17)$$

where τ_{max} indicates maximum possible propagation delay between portable user and receive antenna within an office environment.

IV. SIMULATION RESULTS

In our simulation, a pure LOS MU-MIMO system model is considered. We consider a room of size as depicted in Fig. 3 which has same dimensions as of room GWD119 located in Gillin Hall at the University of New Brunswick (Fredericton,

Canada). We consider a single receiver consisting of two receive antennas and two portable users each having single transmit antenna. The receiver is assumed to be present at the height of 1.6 m above the floor within the center of the room with receiver antenna separation on the scale of carrier wavelength. The portable users are assumed to be present at the same height as that of the receiver but they can move freely to any location within the boundaries of the room. In such a case the maximum separation distance between portable user and receive antenna is calculated to be 6.59 m which leads to a maximum propagation delay of 21.9 ns. Using the relation presented in (17) the average available MU-MIMO bandwidth of an office environment under consideration is approximated to be 45.5 MHz.

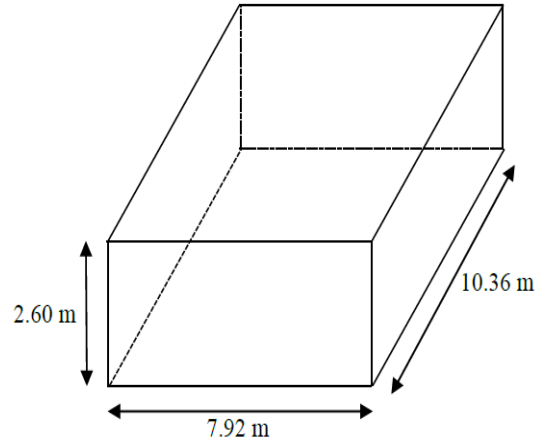


Fig. 3. Size of an office environment under analysis

The proposed system model is implemented with the help of MATLAB[®]. For our simulation results we use 100 random locations for portable users distributed within the boundaries of the room depicted in Fig. 3. Fig. 4 shows the effect of portable user locations on the MU-MIMO bandwidth requirement calculated using equation (16). The results are presented in terms of percentage of portable user locations out of all the locations requiring particular bandwidth. As can be seen in Fig. 4 for 50% of the portable user locations the MU-MIMO bandwidth requirement lie between 300 MHz to 430 MHz. Another 30% of locations contribute to bandwidth requirement that lies between 430 MHz to 640 MHz whereas rest of 20% of the portable user locations contributes to higher bandwidth requirements. This shows the general trend for MU-MIMO system bandwidth requirement for the given office environment. The important point to remember here is that bandwidth requirement is calculated using optimal condition (i.e. condition number equal to one). Therefore, it seems to be more meaningful to present results in terms of condition numbers for different allocated user bandwidths.

In the next simulation, we analyze the effect of allocated user bandwidth on the condition number of the baseband channel matrix. Fig. 5 present results in terms of the percentage of portable user locations that contribute to a particular value of condition number for different allocated user bandwidths. As can be seen in Fig. 5 that as the allocated MU-MIMO bandwidth is increased from 10 MHz to 60 MHz there is a great improvement in the percentage of locations

contributing to lower values of condition numbers. As the allocated bandwidth is increased beyond 60 MHz the improvement in the percentage of locations contributing to lower values of condition numbers start to saturate.

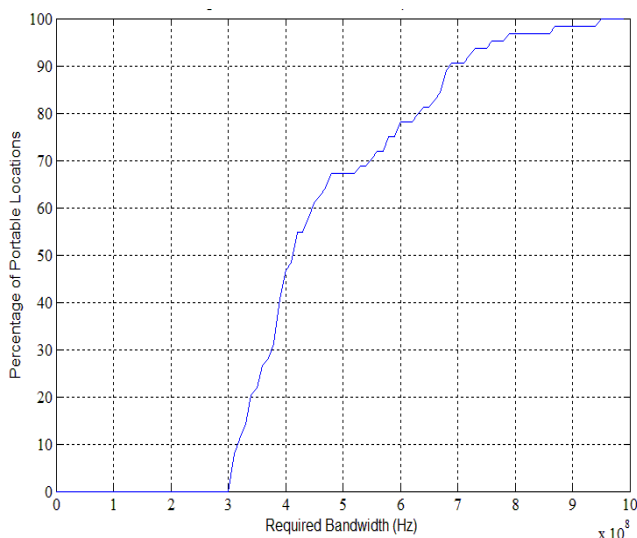


Fig. 4. Bandwidth requirement for different portable user locations

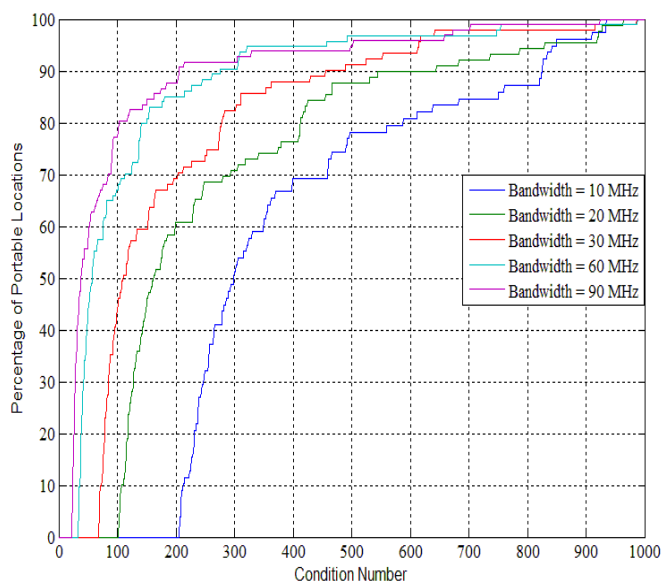


Fig. 5. Resulting condition number for different portable user locations for MATLAB simulation results

The simulation results presented above indicates that:

- If the allocated user bandwidth is less than the predicted average MU-MIMO bandwidth the system performance is degraded.
- Good system performance as well as good bandwidth utilization can be achieved by allocating user bandwidth close to the predicted average MU-MIMO bandwidth.
- If the allocated user bandwidth is greater than the predicted average MU-MIMO bandwidth the system performance is improved but it would result in poor bandwidth utilization.

In the next section, measurement results would be presented to support the analytical and simulation results presented above.

V. MEASUREMENT RESULTS

In this section, results obtained by processing the data collected using prototype MU-MIMO system are presented. The Fig. 6 shows the major components of a prototype system used for measurements. It mainly consists of a computer system for data generation and received data processing. The Altera Stratix II Field Programmable Gate Array (FPGA) development board is used to send generated data in the form of appropriate pulses to the portable users. In addition to this, it is also used to sample the baseband data received from the receiver and send it back to the computer system for further processing.

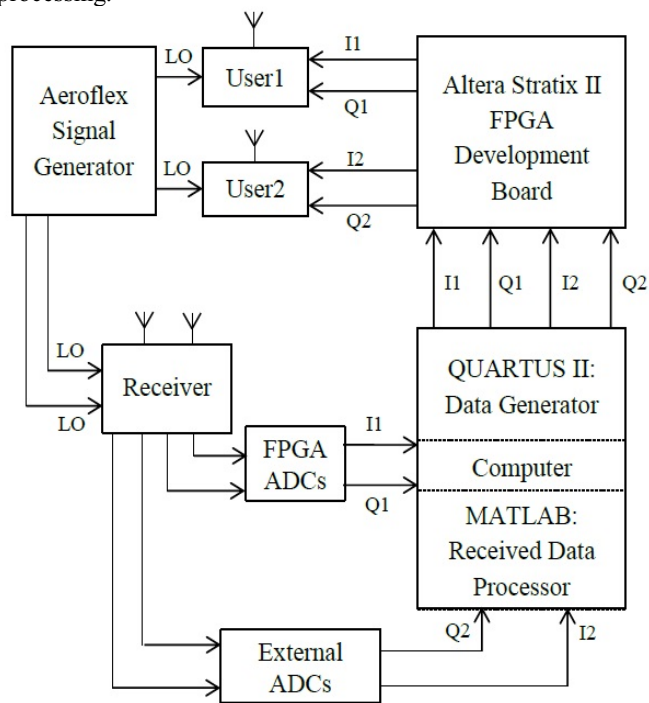


Fig. 6. Prototype MU-MIMO system

The radio frequency band used for measurement results is 1240 MHz – 1300 MHz amateur radio band. Since the maximum available radio frequency bandwidth is 60 MHz and due to the fact that portable users use double sideband modulation; therefore maximum possible baseband bandwidth is 30 MHz. Due to this limitation measurement results would be presented by comparing two different cases of allocated user bandwidth (i.e. allocated bandwidth of 10 MHz and 30 MHz respectively). The room dimensions and other assumptions regarding antenna separation have already been presented in the previous section. As compared to simulation results here we consider only 50 different portable user locations resulting in baseband channel matrix with evenly distributed condition numbers. The Fig. 7 present measurement results for GWD119 for two different cases of allocated user bandwidths. As can be seen in Fig. 7, the measurement results follow the same trend as followed by the simulation results presented in Fig. 5.

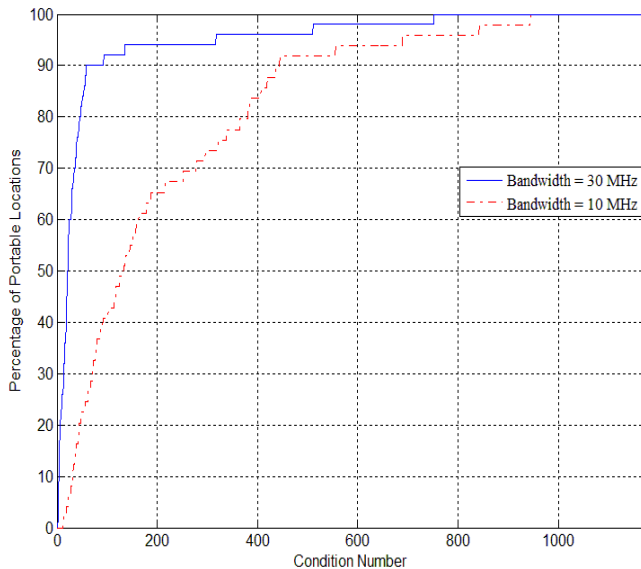


Fig. 7. Resulting condition number for different portable user locations for GWD119 measurement results

Next, we present measurement results for different percentage of area utilizations of room GWD119. Fig. 8 presents results in terms of maximum condition number versus two different allocated user bandwidths (i.e. allocated user bandwidth of 10 MHz and 30 MHz) for different percentage of area utilizations. As can be seen from Fig. 8 for a practical area utilization of 90% of the total area of the room the maximum condition number for allocated bandwidth of 10 MHz is 439 whereas for allocated bandwidth of 30 MHz it is only 59. In addition to this, we can clearly see that as the percentage of area utilization is reduced the change in the condition number for different allocated bandwidths is reduced as well. Therefore a tradeoff exists, for larger percentage of area utilization of particular office environment bandwidth close to the predicted average MU-MIMO bandwidth of an office environment needs to be assigned such that better MU-MIMO system performance is achieved (i.e. lower condition number channel matrix). Allocating lower bandwidth would result in degraded MU-MIMO performance. On the other hand, for lower percentage of area utilization the change in the condition number from lower bandwidth to the average MU-MIMO bandwidth is reduced but the price paid is reduction in the percentage of the area where efficient MU-MIMO system exists.

VI. CONCLUSION

In this paper, we verified the dependence of baseband channel matrix condition number on allocated user bandwidth for LOS MU-MIMO system. The presented hypothesis relates the physical dimensions of an office environment to the average MU-MIMO bandwidth of a given office environment. The presented simulation and measurement results reveal that allocating user bandwidth closer to an estimated average MU-MIMO bandwidth results in existence of an efficient MU-MIMO system over larger percentage of an office space. In addition to this, it also confirms that allocating smaller bandwidths would result in inefficient MU-MIMO system over greater percentage of an office space.

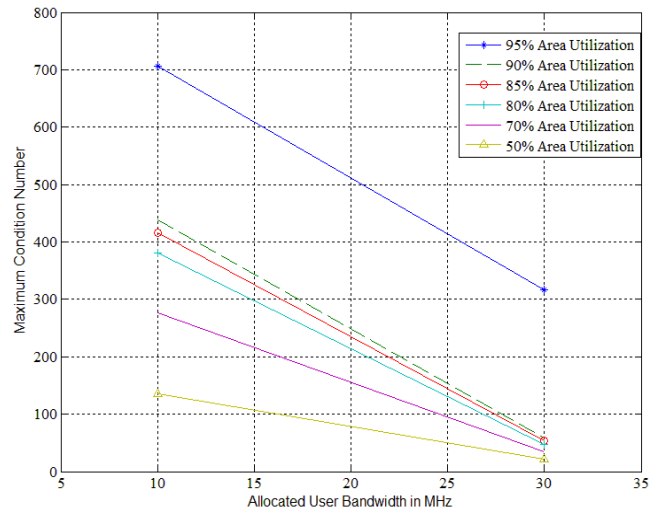


Fig. 8. Area Utilization for different allocated user bandwidths

ACKNOWLEDGMENT

The authors would like to thank the University of New Brunswick, Fredericton for providing financial support to support this research.

REFERENCES

- [1] J. Rasool, G. E. Øien, J. E. Hakegard and T. A. Myrvoll, "On multiuser MIMO capacity benefits in air-to-ground communication for air traffic management," in *Proc. ISWCS*, Siena-Tuscany, Italy, Sept. 7–10, 2009, pp. 458 – 462.
- [2] A. Goldsmith, *Wireless Communications*, 1st ed., New York: Cambridge University Press, 2005.
- [3] A. F. Molisch, *Wireless Communications*, 2nd ed., West Sussex, U.K.: John Wiley & Sons Ltd., 2011.
- [4] B. T. Walkenhorst, "Achieving near-optimal MIMO capacity in a rank-deficient LOS environment," Ph.D. dissertation, Georgia Institute of Technology, Aug. 2009.
- [5] B. Vucetic and J. Yuan, *Space-Time Coding*, 1st ed., West Sussex, U.K.: John Wiley & Sons Ltd., 2003.
- [6] D. Tse and P. Viswanath, *Fundamentals of Wireless Communication*, 5th ed. New York: Cambridge University Press, 2011.
- [7] F. Bohagen, P. Orten and G.E. Øien, "Construction and capacity analysis of high-rank line-of-sight MIMO channels," in *Proc. WCNC*, New Orleans, United States of America, Mar. 13–17, 2005, pp. 432–437.
- [8] G. J. Foschini and M. J. Gans, "On limits of wireless communications in a fading environment when using multiple antennas," *Wireless Personal Communications*, vol. 6, pp. 311 – 335, Mar. 1998.
- [9] G. J. M. Janssen, P. A. Stigter and R. Prasad, "Wideband indoor channel measurements and BER analysis of frequency selective multipath channels at 2.4, 4.75 and 11.5 GHz," *IEEE Trans. Commun.*, vol. 44, no. 10, pp. 1272 – 1288, Oct. 1996.
- [10] G. Zhu, B. R. Petersen and B. G. Colpitts, "Signalling wavelength in an antenna array for space-time wireless over LOS channels," in *Proc. CNSR*, Halifax, Canada, May 16–18, 2005, pp. 69 – 73.
- [11] I. Sarris and A. R. Nix, "Maximum MIMO capacity in line-of-sight," in *Proc. ICICS*, Bangkok, Japan, Dec. 6–9, 2005, pp. 1236 – 1240.
- [12] J. H. Winters, "On the capacity of radio communication systems with diversity in a Rayleigh fading environment," *IEEE J. Select. Areas Commun.*, vol. 5, no. 5, pp. 871 – 878, Jun. 1987.
- [13] J. Shen, Y. Oda, T. Furuno, T. Maruyama and T. Ohya, "A novel approach for capacity improvement of 2 x 2 MIMO in LOS channel using reflectarray," in *Proc. VTC*, Yokohama, Japan, May 15–18, 2011, pp. 1 – 5.
- [14] J. W. Wallace and M. A. Jensen, "Modeling the indoor MIMO wireless channel," *IEEE Trans. Antennas Propag.*, vol. 50, no. 5, pp. 591 – 599, May 2002.

- [15] L. Liu, W. Hong, H. Wang, G. Yang, N. Zhang, H. Zhao, J. Chang, C. Yu, X. Yu, H. Tang, H. Zhu and L. Tian, "Characterization of line-of-sight MIMO channel for fixed wireless communications," *IEEE Antennas Wireless Propag. Lett.*, vol. 6, pp. 36 – 39, Mar. 2007.
- [16] M. A. Jensen and J. W. Wallace, "A review of antennas and propagation for MIMO wireless communications," *IEEE Trans. Antenna Propag.*, vol. 52, no. 11, pp. 2810 – 2824, November 2004.
- [17] S. Yan and Z. Yerong, "Maximum MIMO capacity of rice channel," in *Proc. WCSP*, Nanjing, China, Nov. 13–15, 2009, pp. 1 – 5.
- [18] M. Schwartz, W. R. Bennett and S. Stein, *Communication Systems and Techniques*. Piscataway, NJ: IEEE Press-Wiley, 1995.
- [19] L. W. Hanlen and T. D. Abhayapala, "Space-time-frequency degrees of freedom: fundamental limits for spatial information," in *Proc. ISIT*, Nice, France, June 24-29, 2007, pp. 701 – 705.
- [20] R. Kalbasi, D. D Falconer and A. H. Banihashemi, "Optimum space-time processors with symbol-rate sampling are bandlimited," *IEEE Trans. Signal Processing*, vol. 54, no. 5, pp. 1936 – 1941, May 2006.